

石灰石煅烧过程中产物 CaO 孔隙分布变化研究

王春波, 李永华, 危日光, 陈鸿伟

(华北电力大学 能源与动力工程学院, 河北 保定 071003)

摘要:首次以孔径长度分布函数为基础, 结合比表面积和孔隙率等参数, 建立了石灰石煅烧过程中产物 CaO 孔隙孔径分布模型。并结合实验结果, 对 CaO 孔的分布特性及其受烧结影响而不断演化的过程进行了模拟研究。研究时将 0~50 Å、50~200 Å、200 Å 以上这 3 种孔径范围的孔进行了重点分段分析, 计算表明 3 个孔径范围(0~50 Å、50~200 Å、200 Å 以上)的孔在不同的煅烧阶段对比表面积的贡献是不断发生变化的。在此基础上提出了最佳煅烧率的概念。最佳煅烧率随着煅烧温度的提高而向后推迟。

关键词:石灰石; CaO; 煅烧; 孔径分布; 最佳煅烧率

中图分类号: X701.3 文献标识码: A

1 引言

钙基脱硫剂的孔结构是影响其硫化反应效果的关键因素, 因而, 对其孔结构特性的研究, 一直是人们研究的重点^[1~9]。描述钙基脱硫剂孔结构时, 常用的参数有比表面积、孔隙率和孔径分布等, 其中孔径分布影响最根本。

脱硫剂孔隙的分布反映了各种孔径的孔隙在总孔隙中所占的份额。合理的孔隙分布对优化比表面积、孔隙率及减少硫化过程中不可进入孔的形成都有重要的作用。Gullett & Bruce 等人研究表明^[7], 脱硫剂孔径的有效范围应在 50~200 Å。当孔径小于 50 Å 时, 极易引起孔口闭塞和孔堵塞, 降低脱硫剂的利用率; 当大于 200 Å 时, 可用于硫化反应的孔隙比表面积和孔隙容积会急剧减少; 只有当脱硫剂孔结构的分布合理时, 才能保证脱硫剂具有较高的反应活性。

由于脱硫剂孔结构的非线性, 对其孔径分布的定量描述是非常困难的。因此, 相比于比表面积、孔隙率, 它又是目前人们了解最少的因素, 尽管很多研究者就此做了大量的工作^[7~10]。本文首次以孔径长度分布函数为基础, 结合比表面积和孔隙率等参数, 建立了石灰石煅烧过程中产物 CaO 孔隙孔径分布模型。在实验数据的基础上, 提出了最佳煅烧率这

一概念。

2 孔径分布模型

假设在 CaO 孔隙中不同孔径的孔, 其长度分布是连续的。其长度分布函数 $f(r)$ 可用下式表示^[3]:

$$f(r) = k_1 e^{-k_2 r} \cdot r^3 \quad (1)$$

式中: r —孔半径; k_1 和 k_2 —待定参数。

实际上, CaO 孔的特性是非线性的, 为了便于定量描述, 假设其孔为圆柱状。单位质量 CaO 孔隙中, 孔半径在 $(r, r+dr)$ 的范围内, 所有圆柱孔的总长度应为:

$$dl = f(r) \cdot dr \quad (2)$$

对于圆柱形的孔结构而言, 孔的微元比表面积 ds 和孔隙容积 dv 可分别表示为:

$$ds = 2\pi r dl \quad (3)$$

$$dv = \pi r^2 dl \quad (4)$$

孔半径为 $r \sim dr + r$ 的孔所占全部孔的百分数, 反映了该孔径范围内的孔数目的多少。

$$S_0 = \int_0^\infty 2\pi r \cdot dl \quad (5)$$

$$V_0 = \int_0^\infty \pi r^2 \cdot dl \quad (6)$$

联立式(5)和式(6)得到:

$$\begin{cases} k_1 = 2.5 S_0 / V_0 \\ k_2 = 0.647 6 S_0^6 / V_0^6 \end{cases} \quad (7)$$

若用 CaO 内的总孔隙率 ϵ_0 来表示, 可将总孔隙率 ϵ_0 与孔隙容积 V_0 之间的关系式表示为:

$$V_0 = \frac{\epsilon_0}{\rho_{CaO} (1 - \epsilon_0)} \quad (8)$$

或:

$$\epsilon_0 = \frac{\rho_{CaO} V_0}{1 + \rho_{CaO} V_0} \quad (9)$$

根据确定的 k_1 和 k_2 , 可以计算出任意孔径范围内孔的比表面积 S_r 和孔隙容积 V_r , 即:

$$S_r = \int_{r_1}^{r_2} 2\pi k_1 e^{-k_2 r} \cdot r^4 dr \quad (10)$$

$$V_r = \int_{r_1}^{r_2} \pi k_1 e^{-k_2 r} \cdot r^5 dr \quad (11)$$

3 结果与讨论

利用热太平和压汞仪, 进行了某些工况下脱硫剂孔结构的测试工作。表 1 中所列为 1 073. 15 K, 气氛为空气时煅烧形成的脱硫剂孔隙结构。以下的模拟是以表 1 数据为依据。

表 1 几个典型阶段孔结构

煅烧程度 $X/\%$	比表面积 $S_0/\text{m}^2 \cdot \text{g}^{-1}$	总孔隙率 ϵ_0	孔容积 $V_0/\text{cm}^3 \cdot \text{g}^{-1}$
20	15.1	0.08	0.031 1
40	23.0	0.15	0.063 0
60	29.4	0.20	0.089 3
80	33.2	0.25	0.119 0
100	15.0	0.30	0.138 9

根据孔径分布模型, 模拟计算了石灰石煅烧过程中 0~50 Å、50~200 Å、200 Å 以上的 3 个孔径范围内的比表面积。

图 1 表明, 随着煅烧的进行, 0~50 Å 的孔比表面积先增大, 之后基本上维持不变, 直至煅烧完成 60% 左右时又呈减小趋势。当煅烧完全时, 这些孔基本消失。50~200 Å 的孔比表面积随煅烧进行逐渐增加。当煅烧完成 80% 左右时 50~200 Å 的孔比表面积出现峰值, 而此时 200 Å 以上的孔开始出现并其产生的比表面积逐渐增大。

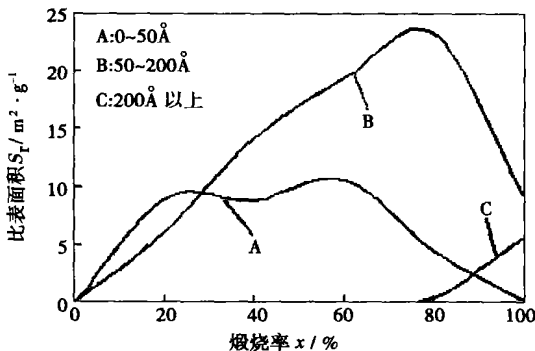


图 1 3 个孔径范围的孔比表面积与煅烧率的关系 (1 073 K)

文献[7]研究表明, 考虑孔阻塞等问题, 孔径处于 50~200 Å 范围内的孔隙对脱硫是最有效的。

基于此结论, 本文定义在石灰石的煅烧过程中,

当孔径为 50~200 Å 的孔对脱硫剂总比表面积的贡献率为最大时的煅烧率, 为最佳煅烧率。此时的煅烧处于最佳煅烧, 所对应的颗粒孔结构为最佳孔结构。在最佳煅烧率时获得的 CaO 具有最好的硫化反应性能。为了得到最佳煅烧率, 对 3 个孔径范围的孔比表面积对总比表面积的贡献率进行了计算 (见图 2)。图 2 计算了它们对总比表面积的贡献率 (按 S_r/S_0 计算) 及其变化趋势。

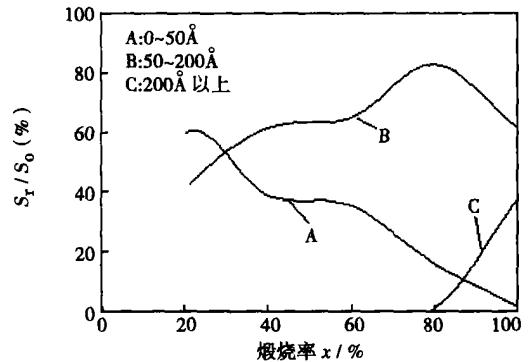


图 2 3 个孔径范围的孔比表面积对总比表面积的贡献率 (1 073 K)

图 2 表明, 在该煅烧工况下, 初始阶段, 0~50 Å 的贡献率相对较大, 随着煅烧的不断进行, 当煅烧进行到 30% 左右时, 50~200 Å 孔的贡献率开始占据主导地位。之后 50~200 Å 孔的贡献率仍保持增长的趋势, 在煅烧率达到 80% 左右时达到峰值, 之后开始下降。同时, 在煅烧完成 80% 以前, 200 Å 以上的孔的对表面积贡献率几乎不存在, 只是在煅烧的最后阶段有所增加。这种趋势和前人实验结果是相符的^[8]。由图 2 还可以发现, 曲线 A 与曲线 C 在煅烧率为 80%~100% 之间出现相交点, 此处所对应的煅烧率即为最佳煅烧率。因为, 此时在孔隙分布密度图上曲线在 50~200 Å 之间所包含的面积为最大。由此可以推测: 当脱硫剂完全煅烧后再参加脱硫反应并不能得到最佳的脱硫效果。如: 当煅烧温度为 1 073 K, 气氛为空气时, 煅烧大约完成 88% 时, 脱硫剂所呈现的孔结构是最有利于脱硫反应的完成。

采用上面的方法, 寻找最佳煅烧率与煅烧条件 (煅烧温度、煅烧气氛等) 的关系, 对于进一步研究脱硫剂脱硫反应将有很大的指导意义。同时, 为了进一步验证模型的准确性, 又选取了两种工况: 973. 15 K 和 1 173. 15 K, 煅烧气氛均为空气时, 对 3 种孔径范围的孔对总的比表面积的贡献率与煅烧率的关系进行了模拟, 如图 3 和图 4 所示。

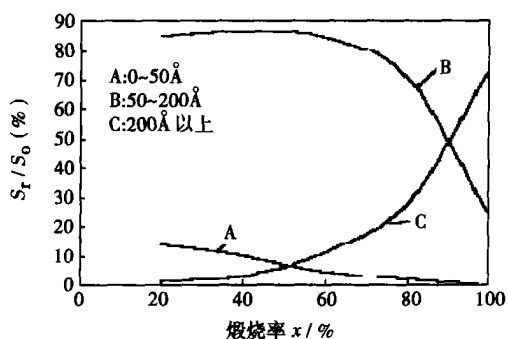


图3 3个孔径范围的孔比表面积对总比表面积的贡献率(973.15 K)

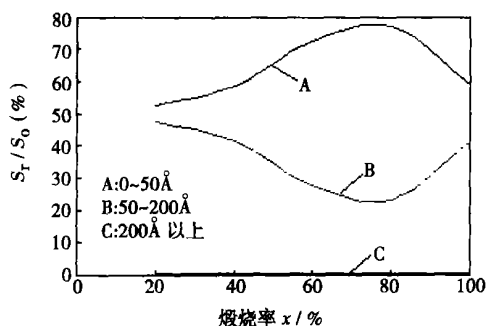


图4 3个孔径范围的孔比表面积对总比表面积的贡献率(1 173.15 K)

对图2~图4进行比较,可以非常明显的看出:不同温度下石灰石煅烧所生成的CaO孔隙分布特性差异是较大的,这可非常明显的由0~50 Å、50~200 Å和200 Å以上的孔所形成的比表面积对总表面积的贡献率反映出来。如图3中,在煅烧完成近70%以前,50~200 Å的孔所占份额基本上保持不变,占了总表面积的80%左右。之后就迅速下降,直到煅烧完全时只占了20%左右。同时,在整个煅烧过程中,200 Å以上的孔的贡献率保持不断的增长直到80%的占有率。当温度为1 173.15 K时,孔结构又呈现出另外的情形:0~50 Å孔的贡献率在整个煅烧过程中都占有绝对优势,而200 Å以上的孔基本不起作用。

由图3可以看出,在973 K的温度下煅烧石灰石时,它的最佳煅烧率大概出现在50%左右,而在1 073 K时又大概出现在88%,但是从1 173 K下煅烧的3个孔径范围的孔比表面积对总比表面积的贡献率图上,却找不到A、C曲线的交点,且此时基本上不出现200 Å以上的孔。但是从图上看出在0~

50 Å的孔出现减小的趋势,而50~200 Å的孔随着煅烧完成时间延长而出现增加的趋势,由此可以预测对于1 173 K温度下的最佳煅烧应该出现在煅烧完全后的某个时间段内。由此推断,最佳煅烧率随着煅烧温度的提高而向后有所推迟。也就是说,对钙基脱硫剂而言,最好的孔结构并不见得是出现在石灰石刚好分解完毕,而可能是出现在煅烧过程中或后的某个阶段。

4 结 论

(1) 3个孔径范围(0~50 Å, 50~200 Å, 200 Å以上)的孔在不同的煅烧阶段对比表面积的贡献是不断发生变化的。

(2) 为了总结孔结构对煅烧的影响,提出最佳煅烧率的概念。最佳煅烧率随着煅烧条件的变化而发生变化,最佳煅烧率随着煅烧温度的提高而向后推迟。在973 K,空气中煅烧时大约出现在煅烧完成50%左右,而在1 073 K,空气中煅烧时推迟到了88%左右,温度提高到1 173 K时,最佳煅烧推迟到完全煅烧之后的某个时刻。

参考文献:

- [1] LAURSEN K. Sulfation and reactivation characteristics of nine limestone[J]. *Fuel* 2000 79(2): 153-163.
- [2] GARCIA LABIANO F. Calcinations of calcium-based sorbents at pressure in a broad range of CO₂ concentrations[J]. *Chem Eng Sci* 2002, 57: 2381-2393.
- [3] DEMIR F. Calcinations kinetic of magnesite from thermo gravimetric data[J]. *Trans IchemE* 2003, 81: 618-622.
- [4] AGNEW J. The simultaneous calcinations and sintering of calcium based sorbents under a combustion atmosphere[J]. *Fuel* 2000 79(12): 1515-1523.
- [5] DIEGO BARLETTA. Modelling the SO₂ limestone reaction under periodically changing oxidizing/reducing conditions: the influence of cycle time on reaction rate[J]. *Chem Eng Sci* 2002, 57: 631-641.
- [6] SOTIRCHOS S V. A distributed pore size and length model for porous media reacting with diminishing porosity[J]. *Chem Eng Sci* 1993, 48: 1487-1502.
- [7] GULLETT B K, BRUCE K R. Pore distribution changes of calcium based sorbents reacting with sulfur dioxide[J]. *AIChEJ*, 1987, 33(10): 1719-1726.
- [8] GUO X Y. Monte carlo simulation of first-order diffusion-limited reaction within three-dimensional porous pellets[J]. *Chinese J Chem Eng* 2003(11): 472-476.
- [9] WENLI DUO, KARIN LAURSEN. Crystalization and fracture; formation of product layers in sulfation of calcined limestone[J]. *Powder Technology*, 2000, 31(3): 154-167.
- [10] FEKKAI S. Fractal dimension segmentation; isolated speech recognition[J]. *Fac of Comp Sci and Engineering* 2000, 12(17): 29-33.

(辉 编辑)

ents, the heat exchange performance and flow resistance characteristics of a single spirally fluted pipe were first studied and a non-dimensional relationship of heat-exchange and flow-resistance characteristics was ascertained. Thereafter, a test tube bundle was made by use of the spirally fluted tubes of the most common specifications currently used on air preheaters of power plants. High temperature air flows inside the tubes, and low temperature air outside the tubes transversely sweeps across the tube bundle. By changing the transverse and longitudinal tube pitch of the staggered tube bundles, a non-dimensional relationship between the Nusselt number and Euler number of each tube bundle on the one hand and various other factors on the other can be obtained. Through an analysis, the tendency of influence exercised by the above-cited transverse and longitudinal tube pitch on the heat-exchange and flow-resistance characteristics can also be revealed. On the basis of the conclusions made from the foregoing, a comparatively rational transverse tube pitch ($S_1=66\text{ mm}$) and longitudinal tube pitch ($S_2=48\text{ mm}$) of the tube bundles may be determined, providing a design basis for the use of spirally fluted tubes in air preheaters and attaining a combined benefit of optimum heat-exchange and flow-resistance characteristics. **Key words:** spirally fluted tube, staggered tube bundle, Nusselt number, Euler number

薄壁蓄热器最大相对温度和最佳切换时间 = Maximal Relative Temperature and Optimum Switching-over Time for a Thin-wall Heat Accumulator [刊, 汉] / AI Yuan-fang, MEI Chi, HUANG Guo-dong, et al (Research Institute of Thermodynamic Equipment Simulation and Optimization under Zhongnan University, Changsha, China, Post Code: 410083) // Journal of Engineering for Thermal Energy & Power. — 2006, 21(4). — 362 ~ 365

A study is conducted of the impact of structural parameters of a thin-wall heat accumulator on its heat transfer performance by using a single parameter perturbation-based semi-analytic numerical calculation method. The research results show that there exists a maximal relative temperature and optimum switching-over time; the maximal relative temperature is directly proportional to the air flow passage length and any change of the circumferential length in the passage can result in a change of the maximal relative temperature; the optimal switching-over time is directly proportional to partition wall thickness. When the wall thickness is 1.0 mm, the optimum switching-over cycle analytic value of 2.5 s is basically in agreement with 4 s of the high temperature gasification intermediate test and 10 s of the low oxygen dispersion-combustion industrial test. The foregoing confirms the feasibility of conducting structural design and operation-and-control optimization of honeycomb-ceramic heat accumulators by use of asymptotic analytic methods. **Key words:** thin-wall heat accumulator, honeycomb-ceramic heat accumulator, maximal relative temperature, optimum switching-over time, semi-analytic numerical method

石灰石的爆裂与磨耗特性研究 = A Study of the Explosive Cracking and Wear Characteristics of Limestone [刊, 汉] / WANG Jin-wei, LI Shao-hua, YANG Hai-ri, et al (Thermal Energy Engineering Department, Tsinghua University, Beijing, China, Post Code: 100084) // Journal of Engineering for Thermal Energy & Power. — 2006, 21(4). — 366 ~ 369

An experimental study was conducted for the explosive cracking. The wear characteristics of limestone of Turkish origin on a fluidized-bed test rig electrically preheated by a small-sized boiler. The calcination temperature and the partial pressure of CO_2 in fluidized media have a very important influence on the explosive cracking of the limestone. When the partial pressure of CO_2 is greater than the equilibrium pressure of limestone decomposition, the calcination reaction will be restrained and the limestone explosive cracking degree is very small. When the partial pressure of CO_2 is smaller than the equilibrium pressure of limestone decomposition, the precipitation of CO_2 produced in the calcination reaction will result in an increase of both the internal pressure and explosive cracking. The particle diameter of calcination products are obviously smaller than that of the original limestone. Moreover, the porosity is also increased by a relatively great degree, which will be conducive to the process of sulfur retention reaction. The calcination product of the limestone has in the fluidized bed the wear characteristics similar to those of coal ash and the wear rate constant basically conforms with the time function of an exponential attenuation. **Key words:** limestone, fluidized bed, explosive cracking, wear

石灰石煅烧过程中产物 CaO 孔隙分布变化研究 = A Study of the Change in Pore Distribution of CaO Produced in the Process of Limestone Calcination [刊, 汉] / WANG Chun-bo, LI Yong-hua, WEI Ri-guang, et al (Energy Source and Power Engineering Institute under the North China University of Electric Power, Baoding, China, Post Code: 071003) // Journal of Engineering for Thermal Energy & Power. — 2006, 21(4). — 370 ~ 372

Based on the distribution function of pore lengths and in combination with such parameters as specific surface area and porosity etc. A pore diameter distribution model was established for the first time for CaO product generated in the process of limestone calcination. In conjunction with experimental results, a simulation study was conducted of CaO pore distribution characteristics and their continuously evolving process when being subjected to the influence of sintering. In the course of the study, a section-by-section analysis has been made with emphasis on the pores with a diameter in the range of 0 ~ 50 Å, 50 ~ 200 Å and over 200 Å. The calculation results indicate that the contribution from the pores in three ranges of pore diameters (0 ~ 50 Å, 50 ~ 200 Å and over 200 Å) to specific surface areas in different calcination stages undergoes a continuous change. On this basis, a concept of optimum calcination rate is proposed, which will take place later with an increase in calcination temperature. **Key words:** limestone, CaO, calcination, pore diameter distribution, optimum calcination rate

添加 CaO 对煤粉燃烧后一次颗粒物特性影响的研究 = A Study of the Effect of CaO Addition on Primary Particle Characteristics after Pulverized Coal Combustion [刊, 汉] / LU Jian-yi, LI Ding-kai (Education Ministry Key Laboratory on Thermal Sciences and Power Engineering under Tsinghua University, Beijing, China, Post Code: 100084) // Journal of Engineering for Thermal Energy & Power. — 2006, 21(4). — 373 ~ 377

A study is made of the effect of CaO addition (3wt%) to pulverized coal on primary particle characteristics after combustion. With a sedimentation furnace serving as a combustion device under an oxidizing atmosphere and combustion temperature of 1100 °C, sample particles after combustion were separated and collected by use of a 8-stage Anderson particle impactor. As seen from the distribution of particle diameters, the addition of CaO to the pulverized coal can reduce the relative amount of fine particles among the primary particles. When Rosin-Rammler distribution function is used to conduct fitting with a particle diameter distribution curve, a very good fitting character has been obtained. As viewed from the emission characteristics, the addition of CaO has reduced the emissions of PM₁₀, PM_{2.5} and PM₁. The SEM image also shows that the particles produced after an addition of CaO contain particle aggregates as a result of merging and clustering. The results of ICP-AES analysis indicate that the content of such heavy metals as Cr, Cu, Ni, Pb and Zn has increased with a decrease in particle diameters. Moreover, when pulverized coal is burned after an addition of CaO, the content of heavy metal elements in the particles has been somewhat reduced. **Key words:** pulverized coal combustion, particle, emission characteristics, heavy metal, additive

大型褐煤锅炉煤粉再燃技术的数值模拟 = Numerical Simulation of Pulverized-coal Reburning Technology for a Large-sized Lignite-fired Boiler [刊, 汉] / TANG Hao, ZHONG Bei-jing, FU Wei-biao (Aeronautics and Astronautics College under Tsing University, Beijing, China, Post Code: 100084), QIU Peng-hua (Energy Source Science and Engineering College under Harbin Institute of Technology, Harbin, China, Post Code: 150001) // Journal of Engineering for Thermal Energy & Power. — 2006, 21(4). — 378 ~ 382

A numerical simulation was conducted of the different combustion air-supply modes for reburning super-fine pulverized coal in an integral furnace of Yuanbaoshan Power Plant No. 3 Boiler on the basis of a dynamic model featuring coal tar NO reduction reaction and by using software Fluent. The numerical simulation results show that a variety of factors, such as the proportion of fuels being reburned, air-coal ratio in the combustion air for reburning and the size of the reburning zone etc. can exercise a major influence on combustion efficiency and NO_x emissions. An optimization calculation has revealed that when the excess air factor in the main combustion zone is controlled at 1.1, a scheme with the following characteristics, namely, the fuel being reburned accounting for 15% of the total fuel amount, coal-air ratio in the combustion air for reburning being set at 2 and the residence time of the flue gas in the reburning zone being about 0.5 s, may be considered as a comparatively well organized mode for reburning. **Key words:** pulverized coal, reburning, numerical simulation

多孔介质内往复流动超绝热燃烧的简化解 = A Simplified Solution for the Super-adiabatic Combustion of Reciprocal Flows in Porous Media [刊, 汉] / SHI Jun-rui, XIE Mao-zhao (Energy Source and Power Engineering College under Dalian University of Science and Technology, Dalian, China, Post Code: 116024) // Journal of Engineering for Thermal Energy & Power. — 2006, 21(4). — 383 ~ 386

A simplified theoretical solution has been obtained through an analogy with stable-state reversed-flow burners followed by a comparison with experimental results. Such a solution is applicable to super-adiabatic combustion in adiabatic inertial po-